



Forces of Change: Optical Tweezers in Membrane Remodeling Studies

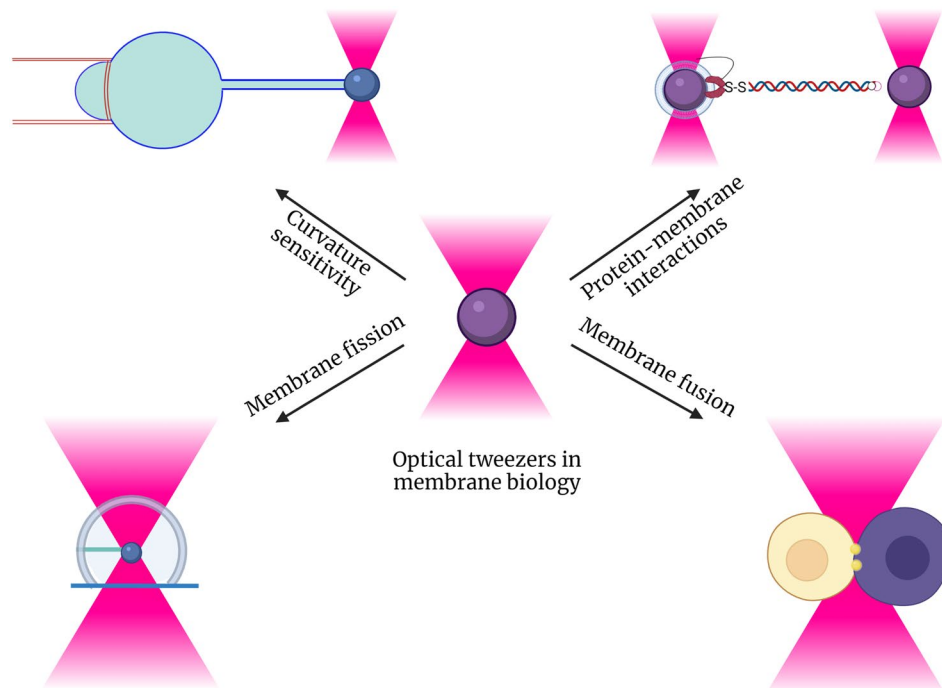
Sudheer K. Cheppali^{1,2,3,4} · Raviv Dharan^{1,2,3,4} · Raya Sorkin^{1,2,3,4}

Received: 28 January 2022 / Accepted: 22 April 2022 / Published online: 26 May 2022
© The Author(s), under exclusive licence to Springer Science+Business Media, LLC, part of Springer Nature 2022

Abstract

Optical tweezers allow precise measurement of forces and distances with piconewton and nanometer precision, and have thus been instrumental in elucidating the mechanistic details of various biological processes. Some examples include the characterization of motor protein activity, studies of protein–DNA interactions, and characterizing protein folding trajectories. The use of optical tweezers (OT) to study membranes is, however, much less abundant. Here, we review biophysical studies of membranes that utilize optical tweezers, with emphasis on various assays that have been developed and their benefits and limitations. First, we discuss assays that employ membrane-coated beads, and overview protein–membrane interactions studies based on manipulation of such beads. We further overview a body of studies that make use of a very powerful experimental tool, the combination of OT, micropipette aspiration, and fluorescence microscopy, that allow detailed studies of membrane curvature generation and sensitivity. Finally, we describe studies focused on membrane fusion and fission. We then summarize the overall progress in the field and outline future directions.

Graphical abstract



Keywords Membrane biophysics · Optical tweezers · Membrane remodeling · Membrane shaping

✉ Raya Sorkin
rsorkin@tauex.tau.ac.il

Extended author information available on the last page of the article

Introduction

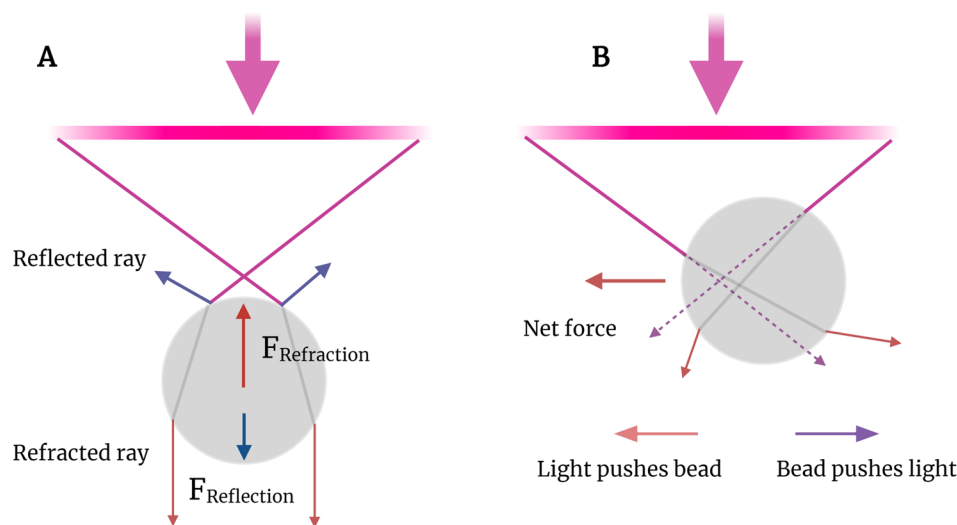
Optical tweezers (OT) have revolutionized biology, as they allow precise manipulation of microscopic objects at time, force, and length scales that are ideally suited for interrogation of biological processes. At the heart of optical trapping lies the interaction of light with matter, resulting radiation pressure. Already in 1619, Johannes Kepler suggested that comets' tails point away from the sun due to pressure induced by light (Kepler 1619). In 1865, James Clerk Maxwell theoretically proved that light could exert radiation pressure along the direction of its propagation (Maxwell 1873). The first experimental demonstration was in 1901 when Pyotr Lebedew, Ernest Fox Nichols, and Gordon Ferrie Hull succeeded to measure the radiation pressure on macroscopic objects using an arc lamp and torsion scale (Lebedew 1901, 1902; Nichols and Hul 1901). The light produced by an arc lamp was incoherent, and so the force it could apply was limited (Ashkin 1970). The invention of lasers, characterized by highly focused and coherent beams, allowed the application of a much higher radiation pressure. Arthur Ashkin was the first to realize that this radiation pressure could be used to push small particles in a liquid environment, and demonstrated that micron-sized beads were drawn toward the center of a laser beam (Ashkin 1970). He later used two counter-propagating beams to cancel out the scattering force, which pushes trapped objects in the direction of light propagation, creating a stable trap. In 1986, using a high numerical aperture objective to focus a single laser beam, he successfully created a three-dimensional optical trap and was able to hold and manipulate microorganisms such as small bacteria and viruses (Ashkin and Dziedzic 1987). This groundbreaking experiment of trapping and manipulating microorganisms without physical contact has

laid the foundation for high-precision optical manipulation of biomolecules.

Physical explanation of optical trapping of an object depends on the size of the object under study in comparison to the wavelength of the trapping laser light (Ashkin et al. 1986). If the size d of the object is such that $d > \lambda$, trapping can be explained based on geometrical or ray optics, while for $d < \lambda$, it can be described by the 'Rayleigh' regime (Ashkin 1992). In the small size limit, the electromagnetic radiation of the light induces a dipole moment in the particle, which is then attracted to the highest intensity point of the beam by the "gradient force" that is proportional to the gradient of the beam intensity. A "scattering force" will act on the particle in the opposing direction to the gradient force, pushing the particle in the direction of the beam propagation. A steep intensity gradient obtained by a high numerical aperture objective allows reaching a balance between these two opposing forces and hence stable trapping. Similarly, a balance of forces is needed for stable trapping in the large size limit (Fig. 1). Here, the reflection of the light pushes the particle forward, similarly to the way a ball bouncing off a box would push it forward. This occurs due to momentum conservation, as the loss of forward momentum by the light results in the gain of such momentum by the particle. Refraction of the light would lead to momentum gain by the refracted beam and thus to restoring force pushing the particle toward the focus. The same principle applies in the lateral direction (Fig. 1). A comprehensive description of optical trapping can be found in other publications (Moffitt et al. 2008; Nieminen et al. 2007; Choudhary et al. 2019; Novotny et al. 1997; Neuman and Block 2004).

Since their development as briefly described above, OT have advanced the understanding of a wide variety of molecular and cellular processes. Studies using optical trapping allowed unraveling motor protein motions and forces (Veigel et al. 2003; Mehta et al. 1999; Schnapp et al. 1990;

Fig. 1 Optical trapping in ray optics regime. **A** The reflected ray results in a force $F_{\text{reflection}}$ pushing the sphere forward, and the refraction of light results in a force $F_{\text{refraction}}$ that pushes the sphere toward the focus. **B** Refraction of rays leads to transverse momentum gain by the light and thus results lateral net force in the opposite direction



Nishizaka et al. 1995), protein folding/unfolding trajectories (Ceccconi et al. 2005; Shank et al. 2010; Stigler et al. 2011), mechanistic aspects of their activities (Gao et al. 2012; Ryu et al. 2015), and mechanical properties of DNA and RNA (Wang et al. 1998; Liphardt et al. 2001) (also reviewed in Nussenzveig 2018; Ritchie and Woodside 2015; Bustamante et al. 2020 and the references therein). Several studies were also carried out on the trapping of specific cellular organelles (Sparkes 2018; Sparkes et al. 2009). Even though optical trapping has been extensively employed with cells and various bio-macromolecules, studies using OT for membrane biophysics-related questions are significantly less abundant, and literature summarizing the overall progress in this field is lacking. Here, we review membrane biophysical studies that utilize OT, with emphasis on various assays that have been developed and their benefits and limitations. First, we discuss assays using membrane-coated beads and overview protein–membrane interactions studies based on the manipulation of such beads. We then describe the most widely used membrane model, giant unilamellar vesicles (GUVs), and studies describing their direct manipulation with OT. Next, we overview a body of studies that make use of a very powerful experimental tool, the combination of OT and micropipette aspiration, together with fluorescent microscopy. This technique, pioneered by Patricia Bassereau and colleagues (Sorre et al. 2009; Ambroggio et al. 2010), allows precise control and manipulation of membrane curvature by modifying the aspiration pressure and thus enables detailed studies of curvature generation and sensitivity. Cellular and intracellular membranes are often characterized by a high area to volume ratio, whereas the generation, modulation, and maintenance of membrane shapes and curved structures are essential for functionality of cells and intracellular organelles. Thus, this technique allows insight into key physiological processes, as we overview in the ‘curvature generation and sensitivity’ section. Finally, we describe studies focused on membrane fusion and fission. We then summarize the overall progress in the field and outline future directions.

Optical Tweezers in Membrane Biophysics

Membrane Model Systems

Various assays have been developed for utilizing OT to interrogate membrane remodeling processes, as covered in detail in the following sections. These studies are conducted using membrane model systems (Sezgin and Schwille 2012; Sezgin 2022), such as supported membranes on polystyrene or silica microbeads (Fig. 2A), GUVs (giant unilamellar vesicles) (Fig. 2B), and very recently, GPMVs (giant plasma membrane vesicles) (Fig. 2C), while one study also

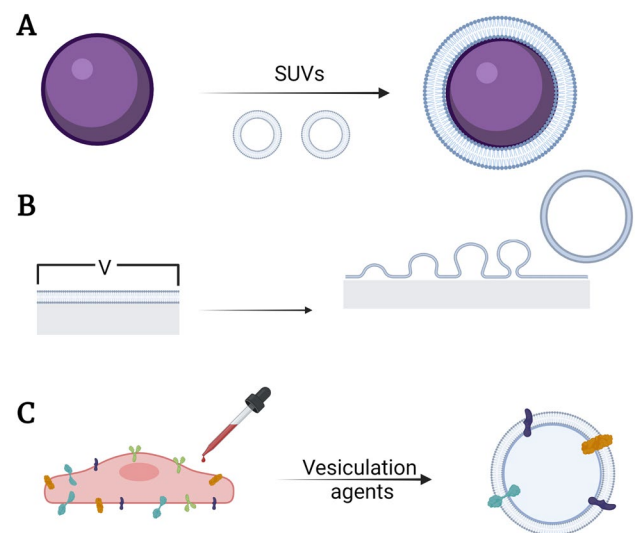


Fig. 2 Membrane model systems used in optical tweezers studies. **A** Microscopic beads coated with small unilamellar vesicles (SUVs). **B** Preparation of giant unilamellar vesicles (GUVs) by electroformation. **C** Preparation of giant plasma membrane vesicles (GPMVs) by induced budding from natural cellular membranes. The cartoons are not to scale

used free-standing membranes (Dols-Perez et al. 2019). We review studies combining these membrane models and optical trapping below.

Supported Lipid Bilayers (SLB) on Microbeads for Studies of Protein–Membrane Interactions

Lipid coating of microspheres is a simple and effective way of creating supported bilayers with tunable and well-controlled lipid composition (Fig. 2A). Supported bilayers can be created by fusing small unilamellar vesicles (SUVs) onto beads. The fusion can be facilitated by the presence of Ca^{2+} ions that can bridge between negatively charged lipid headgroups, like phosphatidylserine (PS), in the bilayer (Brouwer et al. 2015). The efficiency of such membrane coatings is dependent on the salt and liposome concentrations, as increasing salt concentrations resulted in more homogenous membrane coverage (Murray et al. 2016).

One approach to study protein–membrane interactions using OT is by using pairs of optically trapped beads coated with synthetic membranes that are brought into contact and retracted repeatedly in the presence of a soluble protein of interest (or a soluble fragment of a membrane-anchored protein) (Brouwer et al. 2015). This method was employed in studies of membrane remodeling by calcium sensor proteins Doc2b and synaptotagmin-1 (Syt1) (Brouwer et al. 2015; Sorkin et al. 2020) (Fig. 3A & 3B), and provided novel insights into their function. Calcium sensor proteins tightly control the secretion of neurotransmitters

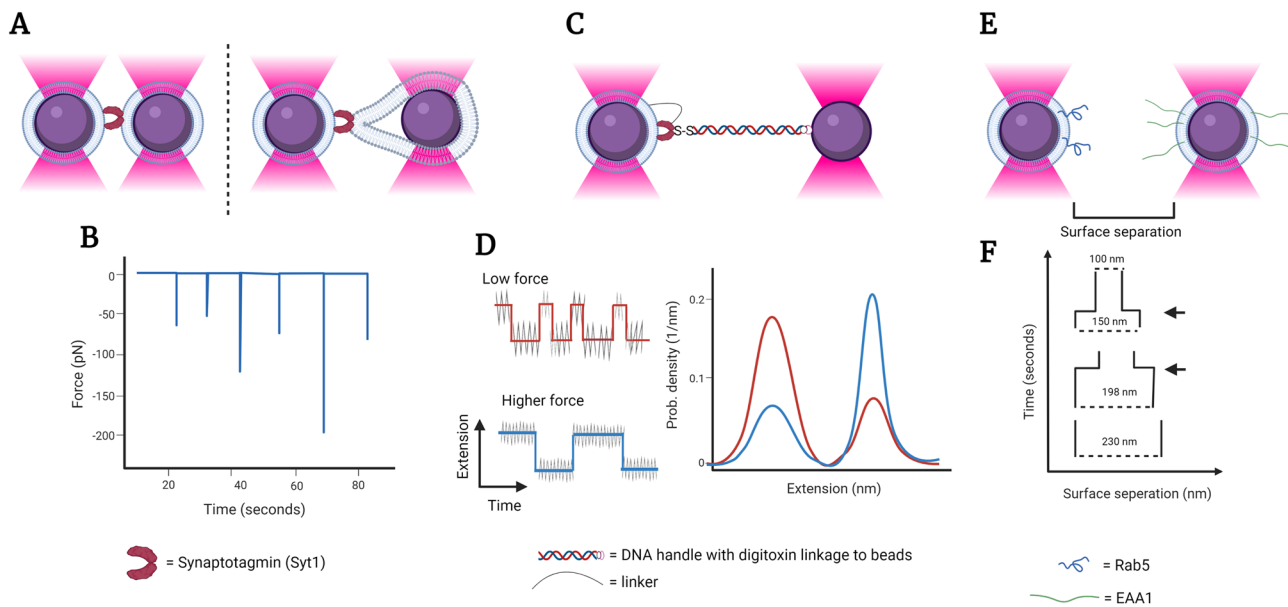


Fig. 3 Various assays investigating protein–membrane interactions using optical tweezers. **A** Experimental scheme where beads coated with synthetic membranes are brought into contact and separated repeatedly in the presence of Syt1. **B** Force–time plot showing the strength of the interactions during a consecutive approach and separation routine as described in (A) (inspired by (Sorkin et al. 2020)). **C** Experimental setup for measuring binding forces between Syt1 and a membrane-coated bead, with a linker that keeps the protein close

to the membrane, thus allowing sequential binding–unbinding transitions. **D** Extension vs. time for the construct in C measured at low and higher forces and the corresponding probabilities of compact and extended states (inspired by (Ma et al. 2017)). **E** Scheme of protein-containing bead-supported membranes. **F** Moving of the trapped beads depicted in E successively closer to one another until interactions occur, leading to increased forces and observed as closer surface separation (shown by arrows). (inspired by (Murray et al. 2016))

and endocrine substances, thus, better understanding of their action mechanisms is of great importance. While multiple studies have been conducted toward this aim and provided critical insights (reviewed in e.g., Rizo 2018; Park and Ryu 2018), open questions still remain regarding the action mechanism of these proteins. The benefit of using correlative OT and fluorescence microscopy to address such questions is that this approach enables one to manipulate single beads/vesicles and measure their interaction forces, with pN precision, concomitantly with fluorescence imaging. This allows employing lipid mixing and content mixing assays to differentiate between three possible membrane interactions scenarios: hemifusion, full fusion, or bridging (without any lipid or content mixing). By using this approach, it was discovered that the calcium sensor Doc2b is able to induce hemifusion between lipid membranes (Brouwer et al. 2015). In a consecutive study, surprising differences were discovered between the action mechanisms of Doc2b and another structurally similar calcium sensor protein, Synaptotagmin-1 (Syt1), which is the key regulator of synchronous neurotransmitter release (Sorkin et al. 2020). One main difference is the preferential arrangement of the protein on the membrane between the symmetric (protein on both beads) and asymmetric (proteins on only one bead) fashion. Syt1 exhibited stronger binding in the asymmetric configuration, whereas Doc2b bound more strongly in the symmetric

configuration, suggesting a preference for Syt1–membrane interaction over Syt1–Syt1 interactions, supporting the ‘direct bridging’ hypothesis (Seven et al. 2013). It was further shown that membrane remodeling by these calcium sensor proteins depends on membrane lipid composition, as cholesterol addition enhanced the probability of membrane hemifusion in the presence of Doc2b, but not with Syt-1 at similar concentrations (Sorkin et al. 2020; Brouwer et al. 2015).

An extensive study of membrane binding energy and kinetics of Syt1 and E-Syt2 (extended synaptotagmin-2) was carried out by Ma et al. (Ma et al. 2017). The authors developed an elegant assay that allows keeping proteins in close proximity to membranes by an extended peptide linker (Fig. 3C and D). Using this assay, reversible protein–membrane binding could be detected based on nm changes in the linker length, with extremely high temporal resolution (10^{-3} – 10^{-4} s). This allowed the authors to derive protein–membrane binding affinity and kinetics as a function of force, soluble factors, and membrane lipid composition. The same assay was used in combination with electrophysiological recordings and revealed that the polybasic patches of both C2A and C2B domains of Syt1 are contributing to membrane binding and are needed for neurotransmitter release (Wu et al. 2021). In another study, surprising differences were found in membrane binding affinities of the C

domains of E-Syt1 and E-Syt2, despite structural similarities (Ge et al. 2022).

Manipulation of membrane-coated beads using OT was also employed in the investigation of membrane tethering during vesicular transport, where tethering means selective docking of transport vesicles to their target membranes prior to fusion of the two bilayers. Vesicles are selectively recognized by their target membranes by a Rab-GTPases regulated process via the recruitment of tethering molecules. Murray et al. looked into the mechanism by which a tethered vesicle comes into contact with its target membrane by several approaches, including an elegant OT assay utilizing reconstituted endosomal tethering machinery (Murray et al. 2016) (Fig. 3E and F). Beads coated with SLB were functionalized with a dimeric coiled-coil protein, EEA1, and using OT, were interacted with beads coated with SLB containing Rab5-GTPase. The separation distance between the two beads was progressively decreased until interactions were observed. It was found that Rab5 binding to EEA1 occurs at an extended conformation of EEA1, and this binding induces a conformational change which leads to a more flexible structure of EEA1, which then collapses and thereby brings the membranes into close proximity to allow fusion. The authors could measure the forces during the tethering reaction and found that the change from extended to the flexible form of the protein generates force up to ~ 3 pN and releases $\sim 14 k_B T$ of mechanical energy (Murray et al. 2016). The authors further suggested that such an entropic collapse upon stiffness reduction could be a general mechanism for generating an attractive force in various biological processes.

GUV/GPMV Manipulation using Optical Tweezers

Giant unilamellar vesicles (GUVs) and giant plasma membrane vesicles (GPMVs) are widely used tools for studies of membrane-associated processes (Dimova and Marques 2019). GUVs are micron-sized synthetic vesicles consisting of a single membrane bilayer. Electroformation is the most commonly used technique to produce GUVs from commercially available lipids (Fig. 2B) due to the high vesicle yield, vesicle unilamellarity, and fewer defects in structure compared to other methods (Angelova and Dimitrov 1986; Bagatolli et al. 2000; Rodriguez et al. 2005). Usually, sugars (mainly sucrose) are added to the interior of GUVs, osmotically balanced by glucose or salts in the outside solution. This causes a difference in refractive indices which allows optical trapping of GUVs, albeit with low trapping force, due to the relatively small contrast in refractive indices. Encapsulating iodixanol within GUVs increases the refractive index difference between GUVs and their medium and thus allows for stronger trapping forces at a given laser power compared with GUVs that encapsulate sugar (Wang et al. 2021). OT can be used to stretch and mechanically

probe GUVs (Solmaz et al. 2012), and can also allow trapping and manipulation of L_o domains on GUVs (Friddin et al. 2019). Such domain manipulation can be useful in sculpting and creating artificial domain patterns (Vivek et al. 2020). OT can also be used to stably trap three-dimensional GUV networks (Bolognesi et al. 2018). GUVs are a popular membrane model system as the biophysical properties of cell membranes are challenging to study due to the constant cellular remodeling and complex interactions with intracellular factors. The GUV model system avoids these challenges, as the membrane composition and buffer conditions within the GUV can be easily controlled, while membrane tension can be manipulated by micropipette aspiration. The integration of micropipette aspiration with OT is a powerful tool that has been used for various assays. Pulling tethers from GUVs allows measuring membrane bending rigidities (Dasgupta et al. 2018), which were found to be in the order of ~ 10 – 30 kT for fluid L_D membranes and above $65 k_B T$ for L_o membranes (Cuvelier et al. 2005, Roux et al. 2005). Additionally, this assay can be used with GUVs that contain reconstituted proteins to study the protein's effect on membrane shape and stiffness (Aimon et al. 2014), as elaborated in the curvature sensitivity section below.

Although GUVs are good models for cell membranes, they have some disadvantages: Incorporating proteins within the membrane usually involves detergents for proper reconstitution. Moreover, while providing controllable membrane composition, the reconstituted model system lacks the complexity of cellular membranes and the essential lateral interactions occurring between proteins and lipids. On the other hand, GPMVs are micron-sized vesicles generated directly from the plasma membrane of cells under stress conditions. GPMVs can be extracted from various cell types (Gerstle et al. 2018) (Fig. 2C) and have the advantage of harboring proteins with their physiological conformation and orientation (Sezgin et al. 2012). GPMVs maintain the compositional complexity of biological membranes, allowing for studies of protein and lipid dynamics and interactions in a near-physiological environment (Moreno-Pescador et al. 2019). The use of GPMVs has become more popular in recent years, and it emerges as a prominent model system for biophysical studies of membranes (Gerstle et al. 2018).

Membrane Curvature Generation and Sensitivity

Membranes of eukaryotes take many shapes, with most intracellular membranes being characterized by a high area to volume ratio. Formation and maintenance of membrane shapes and curved structures are essential for the functionality of cells and intracellular organelles. Local curvature not only provides cells and organelles their shapes, but also affects cellular processes like fusion and fission and the organization of proteins and lipids within the membrane

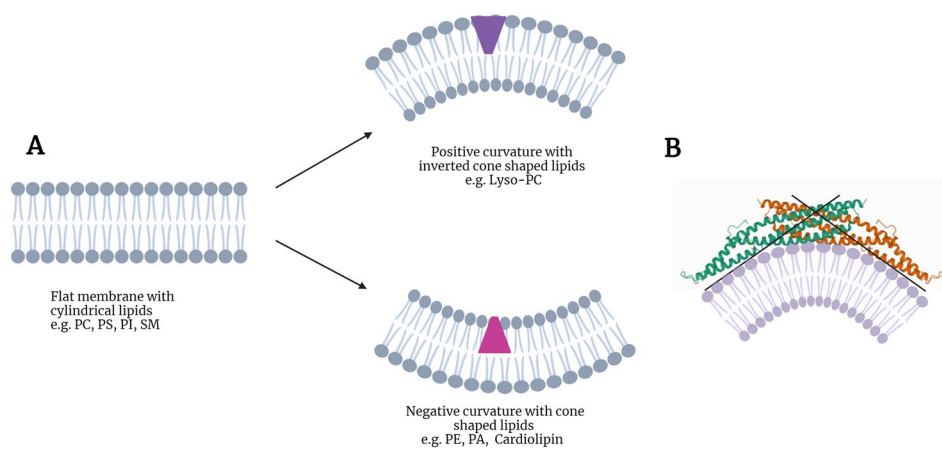


Fig. 4 Membrane curvature. **A** A flat bilayer consisting of cylindrically shaped lipids changes its curvature in the presence of inverted cone-shaped lipids (purple) in the outer monolayer to produce positive curvature, and cone-shaped lipids (pink) in the outer monolayer

to produce negative membrane curvature. **B** Protein-induced membrane curvature. An example of a BAR (Bin/Amphiphysin/Rvs) domain of drosophila amphiphysin (PDB: 1URU) showing preference to membranes with positive curvature (Peter et al. 2004).

(McMahon et al. 2010). Shape generation within biological membranes can be modulated by various mechanisms, such as local changes in the lipid composition and asymmetry, scaffolding by curvature inducing proteins, shallow membrane insertion of hydrophobic protein motifs, and active force application by molecular motors and cytoskeletal filaments (McMahon and Boucrot 2015; Kozlov et al. 2014). Micropipette aspiration combined with optical trapping allows the generation of membrane tethers of varying curvature, thus enabling studies of curvature-induced sorting of various molecules, as elaborated in the following sections.

Lipids

The ability of lipids to undergo curvature-induced sorting has been explored in several studies, motivated by the idea that lipids can potentially have preferred curvature due to their molecular shapes. Lipid molecules have diverse structures that vary in their headgroup type and size as well as acyl chain length and degree of saturation, which dictate their so-called ‘packing parameter’ that affects their mesoscopic assembly preference (Israelachvili 2011) (Fig. 4A). Due to this, when the headgroup is much larger than the tail, as in lysophosphatidylcholine (lyso-PC), lipid molecules have an inverted cone-like shape which promotes positive curvature of the monolayer they reside in. For small headgroup and wide-tail lipids, e.g., phosphatidylethanolamine (PE), phosphatic acid (PA) or cardiolipin (CL), lipid molecules have a conical shape and thus would have negative curvature preference (Fig. 4A). It was found, however, that lipids are generally insensitive to membrane curvature due to their small size (compared to proteins), suggesting that entropy, rather than curvature energy, dominates lipid

distribution (Tian and Baumgart 2009). Curvature-driven lipid sorting can occur at particular conditions, near the demixing point of the system, and is also facilitated by lipid self-association or lipid-clustering proteins (Beltrán-Heredia et al. 2019; Sorre et al. 2009). Sorre et al. (Sorre et al. 2009) showed that the pulling force was lower than expected for tubes pulled from vesicles with a composition close to phase separation, and that this deviation can provide a quantitative measure of lipid sorting. Beltrán-Heredia et al. measured the lipid sorting of cardiolipin at different concentrations and tether curvatures. They estimated its negative intrinsic curvature to be -1.1 nm^{-1} (Beltrán-Heredia et al. 2019), while the sorting of these cone-shaped lipids was found to likely be facilitated by short-range CL–CL attractive interactions. The enrichment of a lipid or protein in the tether vs the vesicle is often defined by the sorting ratio (S):

$$S = \frac{(I_O/I_L)_{\text{tether}}}{(I_O/I_L)_{\text{vesicle}}}$$

where I_O is the intensity of the object (lipid/protein) being examined and I_L is the intensity of lipid dye that is homogeneously distributed on the tether and the vesicle.

GM1, one of the most common gangliosides (lipids with a large saccharidic headgroup) in the brain, is asymmetrically distributed across neuronal membranes and induces membrane shape modifications. In GUVs, higher GM1 concentration in the inner leaflet was found to induce inward tubulation with tubes being stabilized by its negative spontaneous curvature (Dasgupta et al. 2018). The authors were able to estimate this curvature by a combined micropipette aspiration and OT assay, and further demonstrated that membrane curvature can be measured using solely OT

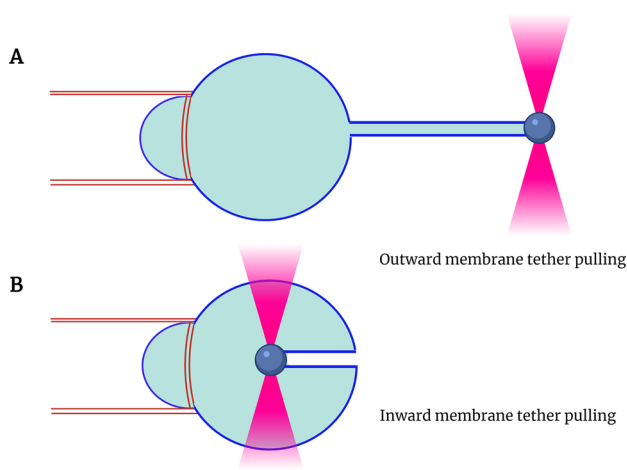


Fig. 5 Membrane tethers pulled from micropipette aspirated GUVs. **A** Outward and **B** inward membrane tether pulled from a GUV using an optically trapped bead. Micropipette aspiration is used to hold the GUV and control its membrane tension by the aspiration pressure (inspired by (Dasgupta et al. 2018))

(without micropipette aspiration) by pulling inward and outward tubes on the same vesicle (Fig. 5). This can be done as follows: the force difference between outward and inward tubes is related to the membrane curvature and bending rigidity via $f_{out} - f_{in} = -8\pi\kappa m$, where f_{out} is the force needed to pull an outward tube, f_{in} is the force needed to pull an inward tube, κ is the membrane bending rigidity, and m is the spontaneous membrane curvature. This is obtained from $f_{out} \approx 2\pi\sqrt{2\kappa\sigma} - 4\pi\kappa m, f_{in} \approx 2\pi\sqrt{2\kappa\sigma} + 4\pi\kappa m$, where σ is the membrane tension, determined by the aspiration pressure, see (Dasgupta et al. 2018) for details. Membrane spontaneous curvature values obtained under various conditions are given in Table 1.

Ions

Several studies examined spontaneous membrane curvature in the presence of different ions. There are contradicting reports regarding the role of Ca^{2+} in curvature generation of negatively charged membranes, with one OT-based study showing that Ca^{2+} generates positive curvature attributed to electrostatic repulsion between Ca^{2+} ions (Simunovic et al. 2015), whereas other studies report negative curvature generation attributed to reduction in the surface charge density on the outer leaflet upon Ca^{2+} binding (Ali Doosti et al. 2017; Graber et al. 2017). The differences in the results may be attributed to differences in the methodologies and experimental conditions, such as membrane composition, Ca^{2+} concentration (which was significantly higher in the positive curvature generation study, thus probably led to repulsion), or differences in salt concentrations which can affect Ca^{2+} binding (Sinn et al. 2006). Monovalent ions can significantly influence Ca^{2+} -induced membrane deformation. For example, high and symmetric Na^+ concentration across the membrane reduces Ca^{2+} binding by electrostatic screening, whereas asymmetric concentration can either oppose or support Ca^{2+} -induced deformation depending on the gradient direction (Graber et al. 2017). The effect of monovalent ions, Na^+ , K^+ and Li^+ on the spontaneous membrane curvature was also studied using OT along with micropipette aspiration (Karimi et al. 2018). Substantial negative spontaneous curvature values were obtained for NaCl and KCl (-8.7 and $-8.5 \mu m^{-1}$, respectively) at high salt concentrations. Li^+ was able to induce negative spontaneous curvature even at lower concentrations. Furthermore, all these ions reduced the membrane bending rigidity (Karimi et al. 2018).

Table 1 Spontaneous membrane curvature (Cm) induced by various molecules/ intrinsic molecular curvature (Cp), measured using optical tweezers

Condition/protein	Spontaneous membrane curvature (Cm)/ Intrinsic molecular curvature (Cp) [nm^{-1}]	References
Cardiolipin	$C_p = 1$	Beltrán-Heredia et al. (2019)
IRSp53 I-BAR domain	$ C_p = 0.055$	Prévost et al. (2015)
Amphiphysin 1	$C_p = 0.111$	Tsai et al. (2021)
Potassium channel protein KvAP	$ C_p = 0.04$	Aimon et al. (2014)
Ca^{2+}	$C_m = 9 \cdot 10^{-3}$	Simunovic et al. (2015)
GM1	$C_m = -1.96 \cdot 10^{-3}$	Dasgupta et al. (2018)
NaCl (28.5 mM)	$C_m = 0.66 \cdot 10^{-3}$	Karimi et al. (2018)
NaCl (142.5 mM)	$C_m = -8.74 \cdot 10^{-3}$	Karimi et al. (2018)
KCl (57 mM)	$C_m = -1 \cdot 10^{-3}$	Karimi et al. (2018)
KCl (142.5 mM)	$C_m = -8.47 \cdot 10^{-3}$	Karimi et al. (2018)
LiCl (28.5 mM)	$C_m = -4.45 \cdot 10^{-3}$	Karimi et al. (2018)

Note that the indicated values apply to the specific conditions of the measurements, such as protein density, as detailed in the publications

Proteins

Several proteins were shown to sense and induce membrane curvature; the potassium channel KvAP was found to partition into nanotubes pulled from GUVs (Aimon et al. 2014). The density of KvAP on tubes having a radius between 15 and 35 nm was on average 3.5 higher than their density on the vesicle, demonstrating the ability of membrane curvature to target proteins to specific locations (Aimon et al. 2014). BAR domain superfamily represents a major class of proteins that can sense and induce membrane curvature (Simunovic et al. 2019). Amphiphysin was found to act as a positive membrane curvature sensor and curvature inducer (Fig. 4B), whereas the strength of curvature sensing and its mechanical effect on membranes depended on the protein density (Sorre et al. 2012). Inverse-BAR domain proteins (I-bar) can sense negative membrane curvature and were found to associate with other proteins such as Ezrin, thereby resulting in their enrichment in curved membranes (Prévoost et al. 2015; Tsai et al. 2018, 2021).

Annexins are a family of membrane proteins that are involved in various physiological processes such as membrane repair, ion channel activity, and vesicle transport. Studies exploring Annexin curvature sensitivity showed that these proteins prefer negative membrane curvature, attributed to their convex-shaped membrane-binding region (Boye et al. 2017, 2018). GPMVs produced from cells expressing Annexins show that they accumulate on the inner leaflet of the membrane (Moreno-Pescador et al. 2019). Variations in the curvature sensitivity of different proteins from this family were observed, with annexin-2 showing no curvature sensitivity, whereas Annexin-5 showed up to 15 times higher sorting to negatively curved tubes compared to the flat GPMV membrane (Moreno-Pescador et al. 2019). Similar sensitivity for negative curvature was observed for Annexin-4 (Florentsen et al. 2021). Membrane tubes pulled from GPMVs containing different Annexins showed different diffusion patterns, correlated to the protein's oligomeric nature. The mobility of Annexin-5 was much higher in the vesicle compared to the tube, suggesting that membrane curvature affects protein–protein interactions (Moreno-Pescador et al. 2019).

The endosomal complex required for transport (ESCRT) machinery comprises more than 30 proteins that catalyze membrane fission (Vietri et al. 2020; Sun et al. 2017; Henne et al. 2011). Encapsulated ESCRT-III proteins such as Snf7, Vps2, and Vps24 within tethers pulled from GUVs demonstrated their negative curvature sensitivity (Schöneberg et al. 2018; De Franceschi et al. 2019a). Other ESCRT-III proteins, however, such as Vps20 and Vps4, can form coats on positively curved or flat membranes (McCullough et al. 2015; Bertin et al. 2020). Membrane tension was also found to be a very important factor in ESCRT proteins recruitment

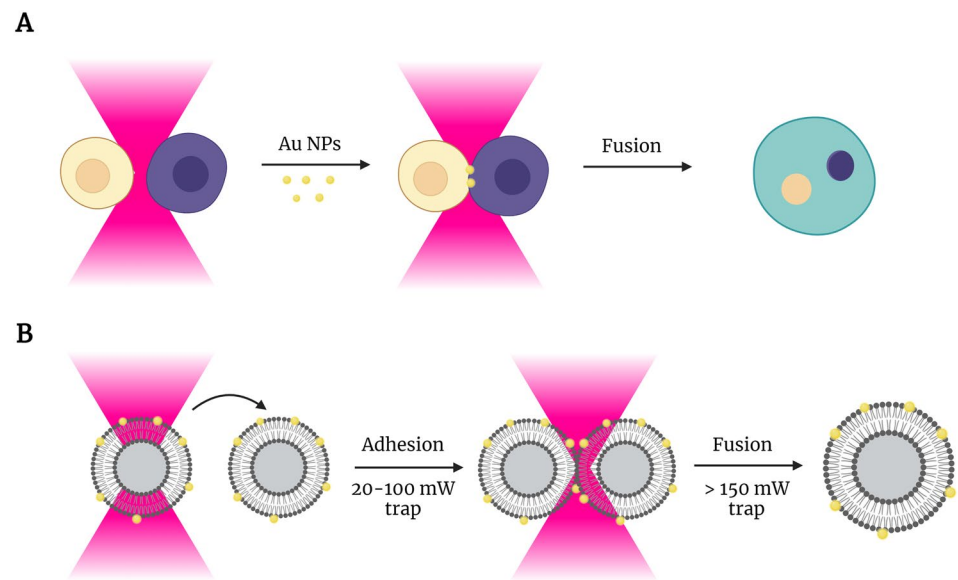
and polymerization; the polymerization of Snf7 was found to be inversely correlated to membrane tension (Mercier et al. 2020). At low tension, it is probably easier for ESCRT proteins to deform the membrane, whereas at high tension, the polymerization energy may not be sufficient for membrane deformation. Together with membrane curvature sensing and membrane deformation, ESCRT proteins facilitate membrane fission, which is further discussed in the ‘Membrane fission’ section below.

Membrane Fusion

Membrane fusion enables multiple physiological processes, such as the function of nerve cells that is enabled by neurotransmitter release by fusion of synaptic vesicles with the plasma membrane at the axon terminal, or cell–cell fusion during fertilization and muscle formation. Membrane fusion does not occur spontaneously and necessitates the action of fusion-promoting proteins called fusogens (Segev et al. 2018). Due to the fundamental importance of membrane fusion, it is extensively studied (Jahn and Scheller 2006; Jahn and Südhof 1999; Jahn et al. 2003; Tang et al. 2020; Brukman et al. 2019; Chernomordik and Kozlov 2003). Many open questions still remain, in particular concerning the action mechanisms of some of the known fusogens as well as the identity of unknown fusogens in other processes. OT in combination with confocal fluorescence can serve as a powerful tool to tackle questions regarding the action mechanisms of fusogens. While a few studies demonstrated hemifusion between bead-supported membranes induced by calcium sensor proteins (Sorkin et al. 2020; Brouwer et al. 2015), such assays have not, so far, been used to study fusogens.

The most abundant use of OT in the context of fusion has so far been for forced membrane fusion by heating. A common method used for optical heating triggered vesicle fusion is trapping a set of GUVs and bringing them in close proximity to one another, then catching a gold nanoparticle and placing it at the boundary between two GUVs. The gold particle absorbs laser radiation and raises the local temperature in its vicinity above 100 °C through heat dissipation (Bendix et al. 2010). The heating of the trapped Au NPs can result in both membrane mixing, indicating hemifusion, and vesicle lumen mixing, indicating full fusion with a stable pore formation (Rørvig-Lund et al. 2015). Optically heated gold nanoparticles were found to induce cell–cell (Fig. 6A), cell–GUV as well as GUV–GUV fusion (Fig. 6B) (Bahadori et al. 2017; Rørvig-Lund et al. 2015). Further, the incorporation of gold nanoparticle–lipid conjugates in the membrane was found to aid not only in fusing GUVs, but also in the fusion of individual lipid domains (Vivek et al. 2020). Several other studies have been carried out where gold nanorods have been used for GUV–GUV OT induced fusion using GUVs with

Fig. 6 Membrane fusion using optically heated gold nanoparticles (Au NPs). **A** Schematic illustration showing fusion between two cells. Both cells were brought close by optical trapping. Injection of Au NPs causes cell–cell fusion, resulting in a single cell with a bigger volume. **B** Adhesion and fusion of GUVs containing Au NP conjugated lipids (Inspired by Bahadori et al. 2017; Vivek et al. 2020)



encapsulated proteins (De Franceschi et al. 2019a, 2019b; Bertin et al. 2020).

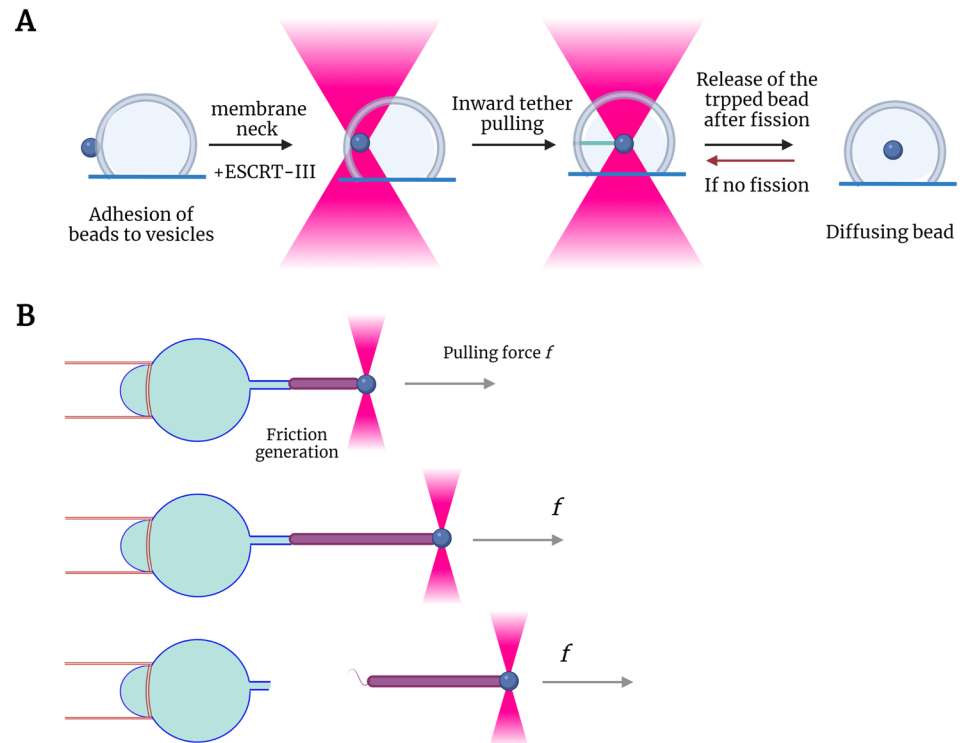
In addition, inferring fusion intermediates from changes in the diffusion of an optically trapped bead that is placed on a supported bilayer has been reported (Keidel et al. 2016). The experiment was conducted with synthetic membranes supported on silica beads. The restriction in positional fluctuations in the z-direction was monitored and reported to decrease with the transition from docking to hemifusion to full fusion. This is, however, a rather indirect method that is not broadly applicable, as diffusion confinement can result from other reasons, e.g., bridging between opposing negatively charged membranes by divalent ions. This assay would thus be more powerful if combined with fluorescence content mixing and lipid mixing assays.

Membrane Fission

Membrane fission is a membrane remodeling process essential for many biological functions. The constriction and scission of membranes during fission is mediated by proteins which act either from the outside of the membrane, such as dynamin (Sweitzer and Hinshaw 1998; Hinshaw and Schmid 1995; Pucadyil and Schmid 2008), or from within the membrane, referred to as ‘reverse topology,’ and mediated by the endosomal complex required for transport (ESCRT) (Henne et al. 2011). ESCRT machinery has a crucial role in various cellular processes, including cell separation during abscission (Elia et al. 2011) and viral budding (Hurley and Hanson 2010). The understanding of the action mechanism of this system has been significantly advanced by using OT bases assays; Chiaruttini et al. found that Snf7, the main component of ESCRT-III, polymerizes into spirals at the surface of lipid bilayers. By allowing polymerization to

occur at the surface of membrane tethers and measuring the forces acting on an optically trapped bead during the polymerization process, the polymerization energy could be estimated. This energy, dependent on the differences in the forces applied before and after polymerization and the membrane bending rigidity, was found to be of relatively high values that are sufficient to induce membrane deformations. Overall, by a combination of several techniques, this study demonstrated that Snf7 filaments can act as spiral springs which are loaded via their polymerization. The release of their compression stress can result in membrane deformation (Chiaruttini et al. 2015). Encapsulation of ESCRT-III components (Snf7, Vps24, and Vps2) with the ATPase Vps4 within GUVs revealed the ATP-dependent force acting on the membrane during scission of a membrane tether held in an optical trap (Schöneberg et al. 2018). Using OT, Pfitzner et al. (Pfitzner et al. 2020) have developed a membrane fission assay to determine the sequence of recruitment events of various proteins of the ESCRTIII complex (Fig. 7A). In this assay, artificial membrane necks are pre-formed by incubating supported GUVs with beads. ESCRT-III proteins in various combinations are then added to the buffer. Next, an inward tether is pulled from the GUV using an optically trapped bead. Upon turning off the laser, one of two scenarios occurs: successful fission of the tether results in free diffusion of the bead within the GUV, whereas a non-fission event leads to the bead returning to the initial position of bead-GUV adhesion. The assay revealed that the right combination of ESCRT-III subunits highly increased the fission efficiency, where the addition of Did2 and Ist1 to the ESCRT-II proteins Vps2, Vps20, Vps24, Vps4/ATP, increased fission efficiency from ~27% to >70% (Pfitzner et al. 2020).

Fig. 7 Membrane fission assays carried out using optical tweezers. **A** ESCRT-III proteins were added to GUVs with pre-formed membrane necks. Fission events can be identified if the bead stays inside the GUV, freely diffusing after release from the trap. **B** Friction mediated membrane scission. Due to friction generated between the membrane scaffold containing BAR proteins (blue) and the bare membrane tube (magenta), membrane scission occurs upon pulling (Inspired from Pfitzner et al. 2020; Simunovic et al. 2017)



Several other proteins involved in membrane fission were studied using OT. FtsZ is a crucial factor in bacterial cell division. Membrane nanotubes pulled from surface-attached GUVs containing FtsZ showed immediate migration of the protein to the tubes, followed by helical deformations of the tubes, indicating dynamic coiling (Ramirez-Diaz et al. 2021). An increase in FtsZ concentration in the tubes increased the coiling and resulted in a ‘spring-like’ compression, which was enhanced by GTPase activity. The mechanical properties of the spring-like structures were measured by inducing lateral oscillations in the GUV and tube position, and recording the force acting on the optically trapped bead. By extracting the force acting on the bead at the applied oscillation frequency, the resistive force of the material per unit length, i.e., the spring constant, was calculated. In the presence of FtsZ, the mean spring constant increased, indicating stiffening of the membrane, and a single FtsZ ring unit was estimated to exert forces in the range of 1 pN upon GTP hydrolysis, which can be sufficient to induce membrane deformation.

A novel friction-mediated scission mechanism was described by Simunovic et al. (Simunovic et al. 2017). They observed that BAR proteins were able to induce membrane scission on dynamically pulled tubes but not on static tubes pulled from GUVs using OT (Fig. 7B). The protein scaffold, bound to the membrane, was able to induce a high frictional barrier for lipid diffusion, and thereby tube elongation generated local membrane tension which promoted

membrane scission through lysis (Simunovic et al. 2017, 2019). A somewhat similar assay was used to study fission by *Drosophila* reticulon, where Rtn11 was found to partition into membrane tubes pulled from silica beads coated with proteo-liposomes. When these nanotubes were pulled, they became increasingly thinner, attributed to a dynamic accumulation of the protein, which amplified constriction. The velocity-dependent constriction of the tethers led to fission, which did not occur in the absence of Rtn11 (Espadas et al. 2019).

The possible role of actin in fission was studied using a biomimetic assay consisting of membrane tethers coated with a polymerized actin network (Allard et al. 2020), as actin is suggested to facilitate fission via, e.g., the friction-driven scission mechanism mentioned above, where actin polymerization might provide the pulling force leading to fission (Simunovic et al. 2017). The authors found, however, that actin had a stabilizing effect on membrane tethers rather than facilitating fission. While pulling tubes coated with actin sleeves did not sever the tube, it resulted in the formation of sections of different radii along the tube, which may contribute to membrane reorganization processes (Allard et al. 2020). Additionally, actin sleeves were found to hinder the mobility of lipids, which is proposed to promote scission (Simunovic et al. 2017).

Conclusions

Optical tweezers have proved as a versatile tool for membrane remodeling and protein–membrane interactions studies, as a multitude of assays that are aimed for probing various aspects of membrane processes were developed. In particular, the powerful combination of OT with micropipette aspiration and fluorescence microscopy provided insight into the processes of membrane curvature modulation and membrane fission. We believe that these tools can also provide insight into membrane fusion, and in particular into the action mechanisms of fusion supporting and mediating proteins, which have been, so far, less explored by these methods. In addition, the use of natural membranes such as GPMVs in OT membrane studies and the development of novel experimental assays, such as tethering schemes that provide the means to unfold membrane proteins, will surely facilitate further contributions of OT-based assays to the understanding of life processes where membrane remodeling plays a crucial role.

Funding RS acknowledges support by the ISRAEL SCIENCE FOUNDATION (Grant No. 1289/20). SKC acknowledges support by the Ratner Center for Single Molecule Science.

Declarations

Conflict of interest S.K.C., R.D. and R.S. declare that they have no conflict of interest.

Ethical approval This article does not contain any studies with animals performed by any of the authors.

References

- Aimon S, Callan-Jones A, Berthaud A, Pinot M, Toombes GES, Bassereau P (2014) Membrane shape modulates transmembrane protein distribution. *Dev Cell* 28:212–218
- Ali Doosti B, Pezeshkian W, Bruhn DS, Ipsen JH, Khandelia H, Jeffries GDM, Lobovkina T (2017) Membrane tubulation in lipid vesicles triggered by the local application of calcium ions. *Langmuir* 33:11010–11017
- Allard A, Bouzid M, Betz T, Simon C, Abou-Ghali M, Lemièrre J, Valentino F, Manzi J, Brochard-Wyart F, Guevorkian K et al (2020) Actin modulates shape and mechanics of tubular membranes. *Sci Adv* 6:3050
- Ambroggio E, Sorre B, Bassereau P, Goud B, Manneville JB, Antonny B (2010) ArfGAP1 generates an Arf1 gradient on continuous lipid membranes displaying flat and curved regions. *EMBO J* 29:292–303
- Angelova MI, Dimitrov DS (1986) Liposome Electro formation. *Faraday Discuss Chem Soc* 81:303–311
- Ashkin A (1970) Acceleration and trapping of particles by radiation pressure. *Phys Rev Lett* 24:156–159
- Ashkin A (1992) Forces of a single-beam gradient laser trap on a dielectric sphere in the ray optics regime. *Biophys J* 61:569–582
- Ashkin A, Dziedzic JM (1987) Optical trapping and manipulation of viruses and bacteria. *Science* 235:1517–1520
- Ashkin A, Dziedzic JM, Bjorkholm JE, Chu S (1986) Observation of a single-beam gradient force optical trap for dielectric particles. *Opt Lett* 11:288–290
- Bagatolli LA, Parasassi T, Gratton E (2000) Giant phospholipid vesicles: Comparison among the whole lipid sample characteristics using different preparation methods - A two photon fluorescence microscopy study. *Chem Phys Lipids* 105:135–147
- Bahadori A, Oddershede LB, Bendix PM (2017) Hot-nanoparticle-mediated fusion of selected cells. *Nano Res* 10:2034–2045
- Beltrán-Heredia E, Tsai FC, Salinas-Almaguer S, Cao FJ, Bassereau P, Monroy F (2019) Membrane curvature induces cardiolipin sorting. *Commun Biol* 2:1–7
- Bendix PM, Reihani SNS, Oddershede LB (2010) Direct measurements of heating Electromagnetically Trapped Gold nanoparticles on supported lipid Bilayers. *ACS Nano* 4:2256–2262
- Bertin A, de Franceschi N, de la Mora E, Maiti S, Alqabandi M, Miguët N, di Cicco A, Roos WH, Mangelot S, Weissenhorn W et al (2020) Human ESCRT-III polymers assemble on positively curved membranes and induce helical membrane tube formation. *Nat Commun* 11:1–13. <https://doi.org/10.1038/s41467-020-16368-5>
- Bolognesi G, Friddin MS, Salehi-Reyhani A, Barlow NE, Brooks NJ, Ces O, Elani Y (2018) Sculpting and fusing biomimetic vesicle networks using optical tweezers. *Nat Commun* 9:1–11
- Boye TL, Maeda K, Pezeshkian W, Sønder SL, Haeger SC, Gerke V, Simonsen AC, Nylandsted J (2017) Annexin A4 and A6 induce membrane curvature and constriction during cell membrane repair. *Nat Commun* 8:1–10. <https://doi.org/10.1038/s41467-017-01743-6>
- Boye TL, Jeppesen JC, Maeda K, Pezeshkian W, Solovyeva V, Nylandsted J, Simonsen AC (2018) Annexins induce curvature on free-edge membranes displaying distinct morphologies. *Sci Rep* 8:1–14. <https://doi.org/10.1038/s41598-018-28481-z>
- Brouwer I, Giniatullina A, Laurens N, Van Weering JRT, Bald D, Wuite GJL, Groffen AJ (2015) Direct quantitative detection of Doc2b-induced hemifusion in optically trapped membranes. *Nat Commun* 6:1–8
- Brukman NG, Uygur B, Podbilewicz B, Chernomordik LV (2019) How cells fuse. *J Cell Biol* 218:1436–1451
- Bustamante C, Bustamante C, Alexander L, MacIuba K, Kaiser CM (2020) Single-Molecule Studies of Protein Folding with Optical Tweezers. *Annu Rev Biochem* 89:443–470
- Cecconi G, Shank EA, Bustamante C, Marqusee S (2005) Biochemistry: Direct observation of the three-state folding of a single protein molecule. *Science* 309:2057–2060
- Chernomordik LV, Kozlov MM (2003) Protein-lipid interplay in fusion and fission of biological membranes. *Annu Rev Biochem* 72:175–207
- Chiaruttini N, Redondo-Morata L, Colom A, Humbert F, Lenz M, Scheuring S, Roux A (2015) Relaxation of Loaded ESCRT-III Spiral Springs Drives Membrane Deformation. *Cell* 163:866–879
- Choudhary D, Mossa A, Jadhav M, Cecconi C (2019) Bio-molecular applications of recent developments in optical tweezers. *Bio-molecules* 9:1–19
- Cuvelier D, Derenyi I, Bassereau P, Nassoy P (2005) Coalescence of membrane tethers: experiments, theory and applications. *Bio-physical J* 88:2714–2726
- Dasgupta R, Miettinen MS, Fricke N, Lipowsky R, Dimova R (2018) The glycolipid GM1 reshapes asymmetric biomembranes and giant vesicles by curvature generation. *Proc Natl Acad Sci U S A* 115:5756–5761

- De Franceschi N, Alqabandi M, Mignet N, Caillat C, Mangenot S, Weissenhorn W, Bassereau P (2019a) The ESCRT protein CHMP2B acts as a diffusion barrier on reconstituted membrane necks. *J Cell Sci* 132:217968
- De Franceschi N, Alqabandi M, Weissenhorn W, Bassereau P (2019b) Dynamic and sequential protein reconstitution on negatively curved membranes by giant vesicles fusion. *Bio-Protoc* 9:1–13
- Dimova R, Marques C (2019) *The Giant vesicle book*. CRC Press <https://www.routledge.com/The-Giant-Vesicle-Book/Dimova-Marques/p/book/9781498752176>.
- Dols-Perez A, Marin V, Amador GJ, Kieffer R, Tam D, Aubin-Tam ME (2019) Artificial cell membranes interfaced with optical tweezers: a versatile microfluidics platform for nanomanipulation and mechanical characterization. *ACS Appl Mater Interfaces* 11:33620–33627
- Elia N, Sougrat R, Spurlin TA, Hurley JH, Lippincott-Schwartz J (2011) Dynamics of endosomal sorting complex required for transport (ESCRT) machinery during cytokinesis and its role in abscission. *Proc Natl Acad Sci U S A* 108:4846–4851
- Espadas J, Pendin D, Bocanegra R, Escalada A, Misticoni G, Trevisan T, Velasco A, Montagna A, Bova S, Ibarra B et al (2019) Dynamic constriction and fission of endoplasmic reticulum membranes by reticulon. *Nat Commun* 10:1–11. <https://doi.org/10.1038/s41467-019-13327-7>
- Florentsen CD, Kamp-Sonne A, Moreno-Pescador G, Pezeshkian W, Hakami Zanjani AA, Khandelia H, Nylandsted J, Bendix PM (2021) Annexin A4 trimers are recruited by high membrane curvatures in giant plasma membrane vesicles. *Soft Matter* 17:308–318
- Fridin MS, Bolognesi G, Salehi-reyhani A, Ces O, Elani Y (2019) Direct manipulation of liquid ordered lipid membrane domains using optical traps. *Commun Chem* 2:1–7. <https://doi.org/10.1038/s42004-018-0101-4>
- Gao Y, Zorman S, Gundersen G, Xi Z, Ma L, Sirinakis G, Rothman JE, Zhang Y (2012) Single reconstituted Neuronal SNARE complexes zipper in three distinct stages. *Nat Chem Biol* 337:1340–1344
- Ge J, Bian X, Ma L, Cai Y, Li Y, Yang J, Karatekin E, De Camilli P, Zhang Y (2022) Stepwise membrane binding of extended synaptotagmins revealed by optical tweezers. *Nat Chem Biol* 18:313–320
- Gerstle Z, Desai R, Veatch SL (2018) Giant plasma membrane vesicles: an experimental tool for probing the effects of drugs and other conditions on membrane domain stability. *Methods Enzymol* 603:129–150
- Graber ZT, Shi Z, Baumgart T (2017) Cations induce shape remodeling of negatively charged phospholipid membranes. *Phys Chem Chem Phys* 19:15285–15295
- Henne WM, Buchkovich NJ, Emr SD (2011) The ESCRT Pathway. *Dev Cell* 21:77–91. <https://doi.org/10.1016/j.devcel.2011.05.015>
- Hinshaw JE, Schmid SL (1995) Dynamins self-assemble into rings suggesting a mechanism for coated vesicle budding. *Nature* 374:190–192
- Hurley JH, Hanson PI (2010) Membrane budding and scission by the ESCRT machinery: It's all in the neck. *Nat Rev Mol Cell Biol* 11:556–566
- Israelachvili JN (2011) *Intermolecular and Surface Forces*, III. Academic press, III
- Jahn R, Scheller RH (2006) SNAREs-engines for membrane fusion. *Nat Rev Mol Cell Biol* 7:631–643
- Jahn R, Südhof TC (1999) membrane fusion and exocytosis. *Annu Rev Biochem* 68:863–911
- Jahn R, Lang T, Südhof TC (2003) Membrane fusion. *Cell* 112:519–533
- Karimi M, Steinkühler J, Roy D, Dasgupta R, Lipowsky R, Dimova R (2018) Asymmetric ionic conditions generate large membrane curvatures. *Nano Lett* 18:7816–7821
- Keidel A, Bartsch TF, Florin EL (2016) Direct observation of intermediate states in model membrane fusion. *Sci Rep* 6:23691
- Kepler J. 1619. *De cometis libelli tres*. I. typis Andrea Apergeri, sumptibus Sebastiani Mylii Bibliopolae Augustani.
- Kozlov MM, Campelo F, Liska N, Chernomordik LV, Marrink SJ, McMahon HT (2014) Mechanisms shaping cell membranes. *Curr Opin Cell Biol* 29:53–60. <https://doi.org/10.1016/j.ceb.2014.03.006>
- Lebedew P (1901) Untersuchungen über die Druckkräfte des Lichtes. *Ann Phys* 311:433–458
- Lebedew P (1902) An experimental investigation of the pressure of light. *Astrophys J* 15:60–62
- Liphardt J, Onoa B, Smith SB, Tinoco II, Bustamante C (2001) Reversible unfolding of single RNA molecules by mechanical force. *Science* 292:733–737
- Ma L, Cai Y, Li Y, Jiao J, Wu Z, Shaughnessy BO, Camilli PD, Karatekin E, Zhang Y (2017) Single-molecule force spectroscopy of protein-membrane interactions. *Elife* 6:1–21
- Maxwell JC (1873) *A treatise on electricity and magnetism*. Clarendon Press, London
- McCullough J, Clippinger AK, Talledge N, Skowrya ML, Saunders MG, Naismith TV, Colf LA, Afonine P, Arthur C, Sundquist WI et al (2015) Structure and membrane remodeling activity of ESCRT-III helical polymers. *Science* 350:1548–1551
- McMahon HT, Boucrot E (2015) Membrane curvature at a glance. *J Cell Sci* 128:1065–1070
- McMahon HT, Kozlov MM, Martens S (2010) Membrane curvature in synaptic vesicle fusion and beyond. *Cell* 140:601–605
- Mehta AD, Rief M, Spudich JA, Smith DA, Simmons RM (1999) Single-molecule biomechanics with optical methods. *Science* 283:1689–1695
- Mercier V, Larios J, Molinard G, Goujon A, Matile S, Gruenberg J, Roux A (2020) Endosomal membrane tension regulates ESCRT-III-dependent intra-luminal vesicle formation. *Nat Cell Biol* 22:947–959
- Moffitt JR, Chemla YR, Smith SB, Bustamante C (2008) Recent advances in optical tweezers. *Annu Rev Biochem* 77:205–228
- Moreno-Pescador G, Florentsen CD, Stbye H, Snder SL, Boye TL, Veje EL, Sonne AK, Semsey S, Nylandsted J, Daniels R et al (2019) Curvature- and phase-induced protein sorting quantified in transfected cell-derived giant vesicles. *ACS Nano* 13:6689–6701
- Murray DH, Jahn M, Lauer J, Avellaneda MJ, Brouilly N, Cezanne A, Morales-Navarrete H, Perini ED, Ferguson C, Lupas AN et al (2016) An endosomal tether undergoes an entropic collapse to bring vesicles together. *Nature* 537:107–111
- Neuman KC, Block SM (2004) Optical trapping. *Rev Sci Instrum* 75:2787–2809
- Nichols EF, Hul GF (1901) A preliminary communication on the pressure of heat and light radiation. *Phys Rev* 13:307–320
- Nieminen TA, Knöner G, Heckenberg NR, Rubinsztein-Dunlop H (2007) Physics of optical tweezers. *Methods Cell Biol* 82:207–236
- Nishizaka T, Miyata H, Yoshikawa H, Ishiwata SKJK (1995) Unbinding force single motor molecule of muscle. *Nature* 377:251–254
- Novotny L, Bian RX, Xie XS (1997) Theory of nanometric optical tweezers. *Phys Rev Lett* 79:645–648
- Nussenzveig HM (2018) Cell membrane biophysics with optical tweezers. *Eur Biophys J* 47:499–514
- Park Y, Ryu JK (2018) Models of synaptotagmin-1 to trigger Ca²⁺-dependent vesicle fusion. *FEBS Lett* 592:3480–3492

- Peter BJ, Kent HM, Mills IG, Vallis Y, Butler PJG, Evans PR, McMahon HT (2004) BAR domains as sensors of membrane curvature: the amphiphysin bar structure. *Science* 303:495–499
- Pfützner AK, Mercier V, Jiang X, Moser von Filseck J, Baum B, Šarić A, Roux A (2020) An ESCRT-III polymerization sequence drives membrane deformation and fission. *Cell* 182:1140–1155.e18
- Prévost C, Zhao H, Manzi J, Lemichez E, Lappalainen P, Callan-Jones A, Bassereau P (2015) IRSp53 senses negative membrane curvature and phase separates along membrane tubules. *Nat Commun* 6:8529
- Pucadyil TJ, Schmid SL (2008) Real-time visualization of dynamin-catalyzed membrane fission and vesicle release. *Cell* 135:1263–1275. <https://doi.org/10.1016/j.cell.2008.11.020>
- Ramirez-Diaz DA, Merino-Salomón A, Meyer F, Heymann M, Rivas G, Bramkamp M, Schwille P (2021) FtsZ induces membrane deformations via torsional stress upon GTP hydrolysis. *Nat Commun* 12:1–11. <https://doi.org/10.1038/s41467-021-23387-3>
- Ritchie DB, Woodside MT (2015) Probing the structural dynamics of proteins and nucleic acids with optical tweezers. *Curr Opin Struct Biol* 34:43–51
- Rizo J (2018) Mechanism of neurotransmitter release coming into focus. *Protein Sci* 27:1364–1391
- Rodríguez N, Pincet F, Cribier S (2005) Giant vesicles formed by gentle hydration and electroformation: A comparison by fluorescence microscopy. *Colloids Surfaces B Biointerfaces* 42:125–130
- Rørvig-Lund A, Bahadori A, Semsey S, Bendix PM, Oddershede LB (2015) Vesicle fusion triggered by optically heated gold nanoparticles. *Nano Lett* 15:4183–4188
- Roux A, Cuvelier D, Nassoy P, Prost J, Bassereau P, Goud B (2005) Role of curvature and phase transition in lipid sorting and fission of membrane tubules. *EMBO J* 24:1537–1545
- Ryu J, Min D, Rah S, Kim SJ, Park Y, Kim H, Hyeon C, Kim HM, Jahn R, Yoon T (2015) Spring-loaded unraveling of a single SNARE complex by NSF in one round of ATP turnover. *Science* 347:1485–1489
- Schnapp B, Block S, Goldstein L (1990) Bead movement by single kinesin molecules studied with optical tweezers. *Nature* 348:348–352
- Schöneberg J, Pavlin MR, Yan S, Righini M, Lee IH, Carlson LA, Bahrami AH, Goldman DH, Ren X, Hummer G et al (2018) ATP-dependent force generation and membrane scission by ESCRT-III and Vps4. *Science* 362:1423–1428
- Segev N, Avinoam O, Podbilewicz B (2018) Fusogens. *Curr Biol* 28:R378–R380
- Seven AB, Brewer KD, Shi L, Jiang QX, Rizo J (2013) Prevalent mechanism of membrane bridging by synaptotagmin-I. *Proc Natl Acad Sci U S A* 110:3243–3252
- Sezgin E (2022) Giant plasma membrane vesicles to study plasma membrane structure and dynamics. *Biochim Biophys Acta - Biomembr* 1864:183857. <https://doi.org/10.1016/j.bbmem.2021.183857>
- Sezgin E, Schwille P (2012) Model membrane platforms to study protein-membrane interactions. *Mol Membr Biol* 29:144–154
- Sezgin E, Kaiser HJ, Baumgart T, Schwille P, Simons K, Levental I (2012) Elucidating membrane structure and protein behavior using giant plasma membrane vesicles. *Nat Protoc* 7:1042–1051
- Shank EA, Cecconi C, Dill JW, Marqusee S, Bustamante C (2010) The folding cooperativity of a protein is controlled by its chain topology. *Nature* 465:637–640
- Simunovic M, Lee KYC, Bassereau P (2015) Screening of the calcium-induced spontaneous curvature of lipid membranes. *Soft Matter* 11:5030–5036
- Simunovic M, Manneville JB, Renard HF, Evergren E, Raghunathan K, Bhatia D, Kenworthy AK, Voth GA, Prost J, McMahon HT et al (2017) Friction mediates scission of tubular membranes scaffolded by BAR proteins. *Cell* 170:172–184.e11
- Simunovic M, Evergren E, Callan-Jones A, Bassereau P (2019) Curving cells inside and out: Roles of BAR domain proteins in membrane shaping and its cellular implications. *Annu Rev Cell Dev Biol* 35:111–129
- Sinn CG, Antonietti M, Dimova R (2006) Binding of calcium to phosphatidylcholine-phosphatidylserine membranes. *Colloids Surfaces A Physicochem Eng Asp* 282–283:410–419
- Solmaz ME, Biswas R, Sankhagowit S, Thompson JR, Mejia CA, Malmstadt N, Povinelli ML (2012) Optical stretching of giant unilamellar vesicles with an integrated dual-beam optical trap. *Biomed Opt Express* 3:2419
- Sorkin R, Marchetti M, Logtenberg E, Piontek MC, Kerklingh E, Brand G, Voleti R, Rizo J, Roos WH, Groffen AJ et al (2020) Synaptotagmin-1 and Doc2b Exhibit Distinct Membrane-Remodeling Mechanisms. *Biophys J* 118:643–656
- Sorre B, Callan-Jones A, Manneville JB, Nassoy P, Joanny JF, Prost J, Goud B, Bassereau P (2009) Curvature-driven lipid sorting needs proximity to a demixing point and is aided by proteins. *Proc Natl Acad Sci U S A* 106:5622–5626
- Sorre B, Callan-Jones A, Manzi J, Goud B, Prost J, Bassereau P, Roux A (2012) Nature of curvature coupling of amphiphysin with membranes depends on its bound density. *Proc Natl Acad Sci U S A* 109:173–178
- Sparkes I (2018) Lessons from optical tweezers: quantifying organelle interactions, dynamics and modelling subcellular events. *Curr Opin Plant Biol* 46:55–61
- Sparkes IA, Ketelaar T, De Ruijter NCA, Hawes C (2009) Grab a golgi: Laser trapping of golgi bodies reveals in vivo interactions with the endoplasmic reticulum. *Traffic* 10:567–571
- Stigler J, Ziegler F, Gieseke A, Gebhardt JCMRM (2011) The complex folding network of single calmodulin molecules. *Science* 334:512–516
- Sun S, Li L, Yang F, Wang X, Fan F, Yang M, Chen C, Li X, Wang HW, Sui SF (2017) Cryo-EM structures of the ATP-bound Vps4E233Q hexamer and its complex with Vta1 at near-atomic resolution. *Nat Commun* 8:16064. <https://doi.org/10.1038/ncomms16064>
- Sweitzer SM, Hinshaw JE (1998) Dynamin undergoes a GTP-dependent conformational change causing vesiculation. *Cell* 93:1021–1029
- Tang T, Bidon M, Jaimes JA, Whittaker GR, Daniel S (2020) Coronavirus membrane fusion mechanism offers a potential target for antiviral development. *Antiviral Res* 178:104792
- Tian A, Baumgart T (2009) Sorting of lipids and proteins in membrane curvature gradients. *Biophys J* 96:2676–2688
- Tsai FC, Bertin A, Bousquet H, Manzi J, Senju Y, Tsai MC, Picas L, Miserey-Lenkei S, Lappalainen P, Lemichez E, Coudrier E (2018) Ezrin enrichment on curved membranes requires a specific conformation or interaction with a curvature-sensitive partner. *Elife* 7:e37262. <https://doi.org/10.7554/eLife.37262>
- Tsai FC, Simunovic M, Sorre B, Bertin A, Manzi J, Callan-Jones A, Bassereau P (2021) Comparing physical mechanisms for membrane curvature-driven sorting of BAR-domain proteins. *Soft Matter* 17:4254–4265. <https://doi.org/10.7554/eLife.37262>
- Veigel C, Molloy JE, Schmitz S, Kendrick-Jones J (2003) Load-dependent kinetics of force production by smooth muscle myosin measured with optical tweezers. *Nat Cell Biol* 5:980–986

- Vietri M, Radulovic M, Stenmark H (2020) The many functions of ESCRTs. *Nat Rev Mol Cell Biol* 21:25–42. <https://doi.org/10.1038/s41580-019-0177-4>
- Vivek A, Bolognesi G, Elani Y (2020) Fusing artificial cell compartments and lipid domains using optical traps: A tool to modulate membrane composition and phase behaviour. *Micromachines* 11:388
- Wang MD, Schnitzer MJ, Yin H, Landick R, Gelles J, Block SM (1998) Force and velocity measured for single molecules of RNA polymerase. *Science* 282:902–908
- Wang Y, Kumar A, Jin H, Zhang Y (2021) Single-molecule manipulation of macromolecules on GUV or SUV membranes using high-resolution optical tweezers. *Biophys J* 120:5454–5465
- Wu Z, Ma L, Courtney NA, Zhu J, Zhang Y, Karatekin E (2021) Polybasic patches in both C2 domains of Synaptotagmin-1 are required for evoked neurotransmitter release. *bioRxiv*. <https://doi.org/10.1101/2021.07.05.451149>

Publisher's Note Springer Nature remains neutral with regard to jurisdictional claims in published maps and institutional affiliations.

Authors and Affiliations

Sudheer K. Cheppali^{1,2,3,4} · Raviv Dharan^{1,2,3,4} · Raya Sorkin^{1,2,3,4} 

¹ Raymond and Beverly Sackler Faculty of Exact Sciences, School of Chemistry, Tel Aviv University, Tel Aviv, Israel

² Center for Physics and Chemistry of Living Systems, Tel Aviv University, Tel Aviv, Israel

³ Center for Nanoscience and Nanotechnology, Tel Aviv University, Tel Aviv, Israel

⁴ Center for Light-Matter Interaction, Tel Aviv University, Tel Aviv, Israel